Mine Fill 2014 – Y Potvin and AG Grice (eds)

doi:10.36487/ACG_rep/1404_40_Mohanty

Blast vibration monitoring in cemented paste backfill during its curing stage – a case study

B Mohanty *University of Toronto, Canada*

LF Trivino *University of Toronto, Canada*

Abstract

An extensive seismic monitoring program was carried out at an underground mine as part of a comprehensive geotechnical study on the behaviour of cemented paste backfill (CPB) used as stope filling material, under a normal production blast environment. The ultimate goal of the study was to investigate potential liquefaction hazard of CPB due to seismic vibrations issuing from nearby blasting operations. The specific objectives of this phase of the investigation were to; (a) characterise the seismic response of both in situ rock and CPB in selected areas as it relates to normal blasting operation in the mine, (b) determine both amplitude and frequency characteristics of the vibrations issuing from both controlled and normal production blasts in the vicinity of backfilled stope, and (c) study the effect of curing time on the vibration characteristics in the backfill. Multiple vibrations sensors in the form of triaxial accelerometers were embedded in both in situ rock and adjacent backfill. The accelerometers employed in the backfill had a maximum amplitude range of 5-10 g and a frequency response of 1-5 kHz; the accelerometers in rock had a maximum range of either 500 or 1,000 g and a frequency range of 1-10 kHz. The range of distance employed from the blasts was 10-100 m. This paper details the changes in the blast vibration characteristics in CPB with curing time (up to 28 days) in terms of vibration amplitude, frequency content, and the changes in both P-wave velocity, and their implication on vibration loads from typical production blasts at the mine.

1 Introduction

The use of appropriate backfill is an integral part of all underground mining operations. Consequently, a range of practice and backfill compositions are widely used. However, quantitative analysis and monitoring the response of CPB to normal production blasting operations (and to mining-induced micro-seismic and rockburst events) has been far less extensive than required. The major concern in this case is the integrity of CPB, especially during its curing stage, due to dynamic loading directly related to the imposed vibration levels from these events. This has serious implications on potential liquefaction of the backfill, especially during its curing phase.

Monotonic triaxial tests on CPB specimens (Aref 1989) showed a dilative response, indicating that CPB may not be susceptible to liquefaction. Similarly, undrained triaxial compression tests carried out by Been et al. (2002) showed dilative behaviour with no significant change of pore pressure during monotonic loading. In contrast, le Roux et al. (2004) showed that although 12 h cured CPB with 5% binder content did not indicate liquefaction potential, the same CPB with 3 h of curing time was susceptible to cyclic liquefaction. They also showed that the behaviour of 3 h cured CPB was similar to that of non-plastic silt.

In terms of strength, CPB typically has a significantly lower strength than its surrounding rock mass. Previous studies have shown that while the unconfined compressive strength (UCS) of a rock mass may vary from 5-240 MPa, typical UCS in CPB varies from 0.2-4 MPa (Grice 1998; Revell 2000). Grabinsky et al. (2008) and Saebimogadan (2010) reported UCS values of in situ sampled, nine month cured CPB (3% binder composed of 50% Portland cement (PC) and 50% fly ash) of up to only 0.3 MPa.

The dynamic response of silty sand CPB was investigated by Johnson et al. (2007) through Split-Hopkinson pressure bar (SHPB) tests, motivated by rockburst observations (up to 3.5 magnitude) at the Galena mine. Although the tests conducted were not appropriate to evaluate liquefaction potential, they showed that

the dynamic compressive strength of 28 h cured samples was about twice the quasi-static UCS. They also showed that only about 5% of the supplied energy was absorbed by the specimens, while the remaining 95% was reflected. Studer and Kok (1980) studied the response of CPB to blasting in terms of pore water pressure. They categorised pore water pressure in three groups; (i) hydrostatic, (ii) dynamic, related to stress wave amplitude, and (iii) residual, controlled by load intensity and soil conditions.

Mohanty et al. (1995) carried out the initial studies in characterising vibration levels as recorded in CPB due to normal production blasting operations. Through systematic monitoring, they developed an empirical relation between ppv in CPB as a function of scaled distance, i.e. a combination of distance and weight of explosive, in backfill during vertical crater retreat (VCR) blasting at Crean Hill Mine, Ontario, and Canada. ppv can of course be used to calculate the dynamic load, as a first step, imposed on CPB during normal blasting operations.

2 Experimental study at an underground mine

A comprehensive blast monitoring program was carried out at an underground base metal mine in order to characterise the generated blast induced seismicity and the behaviour of CPB. The content of cement in CPB in Canadian mines varies typically between 3 and 6.5% of the solid mass (Ouellet et al. 1998). Additionally, CPB blends may include a combination of PC slag, PC fly ash and sand. Typical compositions of CPB used at this particular operation are shown in Table 1.

Table 1 CPB composition

Component	Plug	Main
Aggregates, A	46%	47%
Binder, B	4%	2%
Tailings, T	50%	51%
Total mass, A + B + T (t)	8,850	12,880
Added water (% of A + B + T)	3.3%	2.6%

The investigation at the mine included detailed investigation of the seismic transmission and response characteristics in both in situ rock and CPB to vibrations produced by blasting operations at the mine.

A total of six triaxial accelerometer stations were installed in rock (three stations) and CPB (three stations) to monitor blast vibrations from single and mult-hole blasts. Typical assembled transducers ready to be installed in rock (grouted in-hole) and CPB (as part of instrumentation clusters to be inserted into the stope to be backfilled) are shown in Figure 1.

The blasting program was divided in two parts: monitoring a single charge of explosive (single-hole blasts), and production blasts with multiple holes. Figure 2 shows the geometry of the test area, indicating the location of accelerometer stations, single-hole charges and the production blast stope. The accelerometers in rock had a specified maximum amplitude of either 500 or 1,000 g and a flat response to frequencies in the range of 1-10 kHz (with ±5% of accuracy). They were grouted in the boreholes with the orientations of the triaxial sensors was carefully controlled. In CPB, triaxial accelerometers with ranges of ±5 and ±10 g were used, with frequency ranges of 1-3 and 1-5 kHz, respectively (with ±5% of accuracy).

The accelerometer data was recorded on both high-speed multi-channel magnetic data acquisition systems (40 kHz bandwidth) and digital data acquisition system (typically 100 kHz of sampling rate), with a total capacity of up to 48 channels. Some of the key accelerometers stations were recorded at multiple gain settings so as to record data with the maximum signal-to-noise ratio.

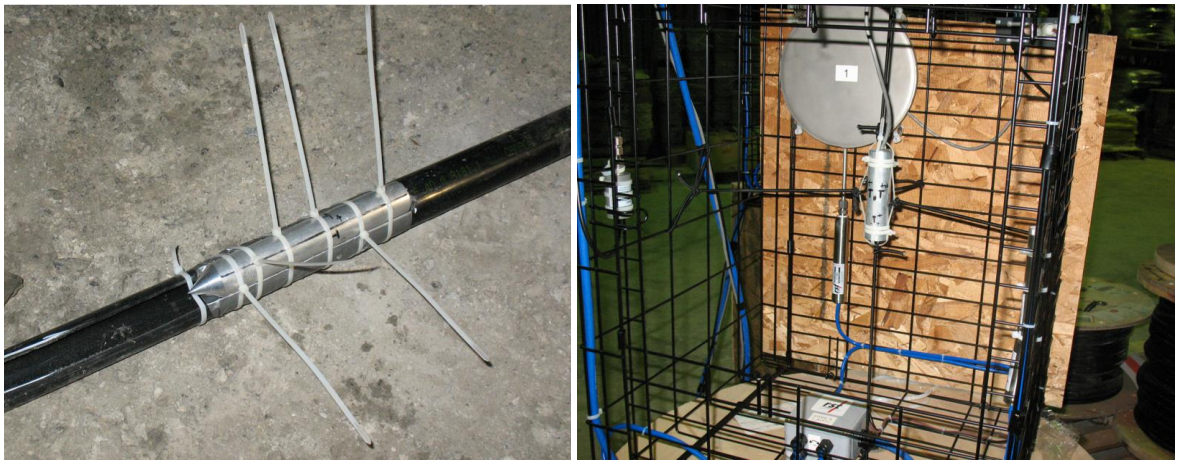

(a) (b)

Figure 1 Triaxial accelerometers with controlled orientation; (a) ready to be grouted in rock; and (b) ready to be inserted in stope to be backfilled

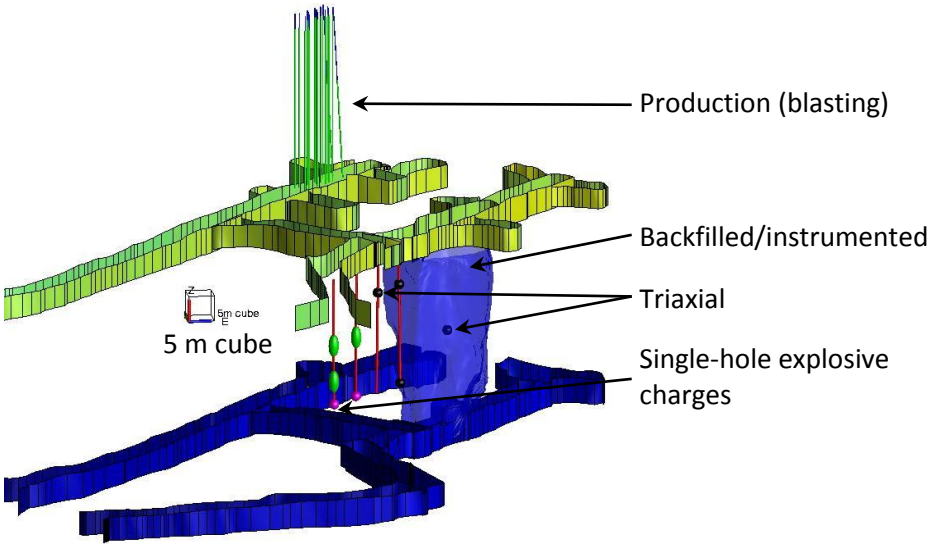

Figure 2 Underground geometry and sensor layout; instrumented stope is located between levels 8700 and 8800 (depth in feet); production stope is located one level above (8600-8700)

2.1 Single-hole and multi-hole production blasts

A total of five single-hole blasts (also referred to as control blasts) were executed. In all cases the explosive type used was water gel in cartridges. All the holes were loaded by gravity into a 114 mm diameter hole, and no stemming or sealing material was used below or above the explosive, however, in all cases the blastholes were flooded. All the blasts were initiated with shock tube detonators. 'Direct', 'reverse' and 'middle' priming methods were employed to study their respective effects on energy release (i.e. vibration characteristics). The vibrations from a multi hole production blast were monitored with multiple accelerometer stations. The blast corresponded to a stope production located about 50 m from the instrumented stope (Figure 2). Eighteen holes were loaded with water gel explosives, and the amount of explosive per delay (per hole) varied from 270-450 kg (total 7,580 kg). The blast was initiated with electronic detonators.

3 Experimental results

The recorded vibration data was analysed in terms of particle velocity in both rock and CPB. The acceleration data was converted to particle velocity data through numerical integration. However, in such conversions, any DC (direct current) drift in the acceleration record often adds significant error to particle velocity values. As is common practice, a numerical filter was applied during the integration process to eliminate this effect. In the present case, 20 and 100 Hz sharp low-pass Butterworth filters were applied to CPB and rock data respectively.

3.1 Control blasts

For the analysis of seismic signals, the vectors of motion (particle velocity in this case) are expressed in spherical coordinates with origin at the centre of the explosive charge. Unless otherwise stated, the signals and frequency analysis presented in this paper correspond to the radial component, which typically contains the highest amplitude in terms of both acceleration and velocity. In order to compare the frequency content of signals the analysis is carried out in terms of average frequency calculated according to the following expression:

$$\bar{f} = \frac{\sum f_i \cdot A(f_i)}{\sum A(f_i)} \quad (1)$$

Where $\bar{f}$ is the average frequency (Hz), f_i represents the individual frequencies in the spectrum (Hz), and $A(f_i)$ is the amplitude associated with each frequency f_i. In order to prevent noise from severely affecting the average frequency, only frequencies with amplitudes of at least 20% of the maximum amplitude in the spectrum were considered to calculate the average.

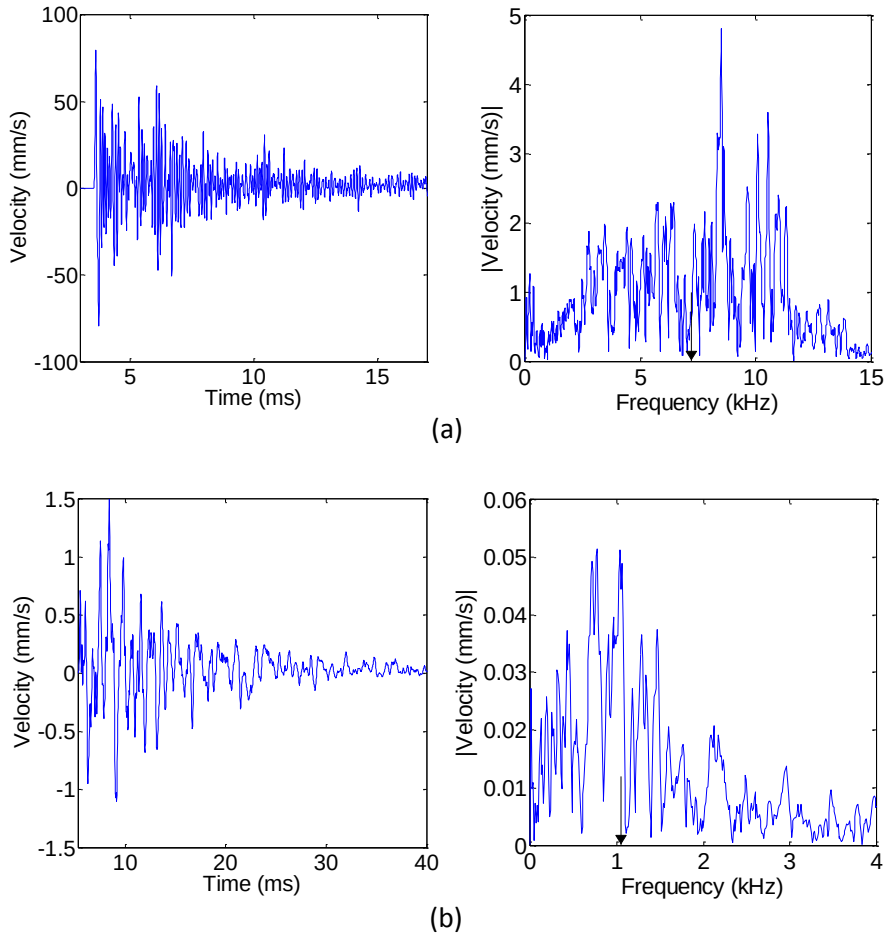

Figure 3 Velocity time history and amplitude spectra (radial component) for a short charge (2.03 kg) of water gel explosive (water-coupled); (a) rock, 21.2 m distance source-sensor; (b) CPB, 2.8 day curing time, 23.5 m distance source-sensor

Figure 3 shows the radial component of velocity time histories and respective frequency spectra recorded in rock and CPB (2.8 days curing time) from short (2.03 kg explosive) single-hole blasts. Despite the similar distances between explosive centre and sensors (21.2 and 23.5 m), the signals show dramatic differences in terms of both amplitude and frequency content. In terms of amplitude the ppv decreases from 80 mm/s in rock to 1.5 mm/s in CPB, while the average frequency (indicated by arrows in the amplitude spectra) drops from 7.2 kHz in rock to 1 kHz in CPB.

Figure 4 shows the results of velocity and frequency spectra for a long explosive charge (34.5 kg). In this case, the frequency content of the signal recorded in rock shows severe attenuation of frequencies greater than 6 kHz. As in the case of a short charge (Figure 3), CPB greatly attenuates the signals compared to that in rock and most of the energy is concentrated in frequencies below 1 kHz.

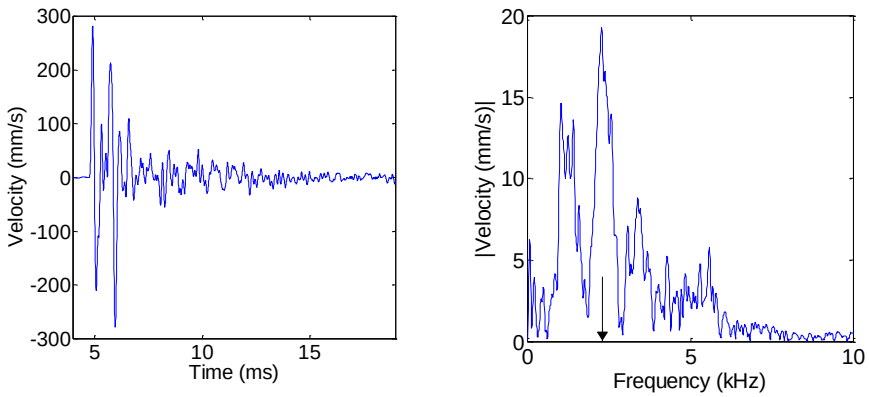

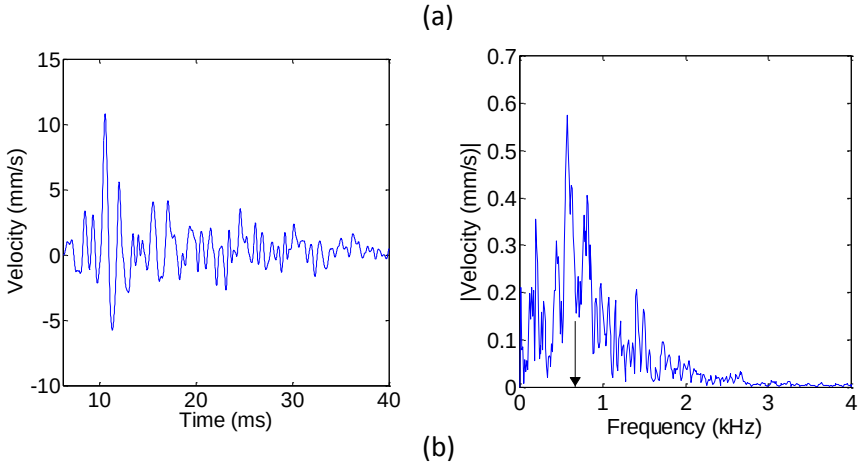

Figure 4 Velocity time history and amplitude spectra (radial component) for a long charge (34.5 kg) of water gel explosive (water-coupled); (a) rock, 26.2 m distance source-sensor; (b) CPB, 24.5 day curing time, 31.9 m distance source-sensor

3.2 Production blasts

Similar to single-hole blasts, the analysis presented here corresponds to the radial component, *r'*, which in this case is taken from the centre of gravity of all the blastholes of the production blast to the observation point (sensor). Figure 5 shows particle velocity time histories recorded in rock and CPB, while Figure 6 shows the first signal in the sequence amplified along with the corresponding amplitude spectra. The same drastic reduction in amplitude in CPB compared to rock obtained from single-hole blasts is not observed in the production blasts. While the frequency spectra show a decrease of frequencies with highest energy by a factor between four and eight, the decrease in maximum amplitude is only by a factor of three. This is to be expected however, as the distances concerned are nearly three times greater than in the single-hole case, with the attendant attenuation of both parameters in rock, where the higher frequency signals were absent to start with.

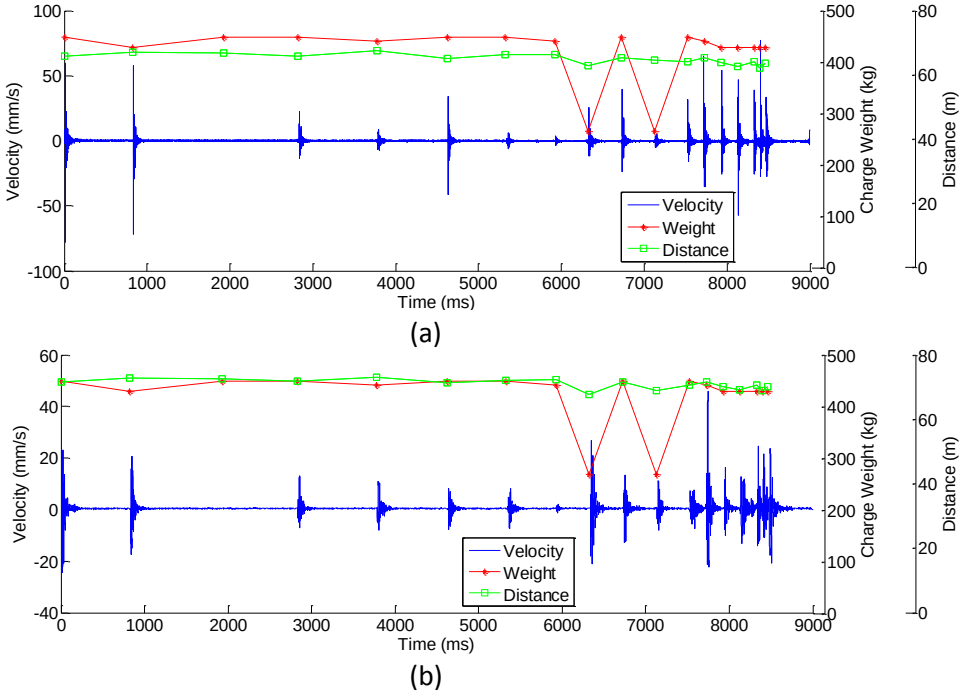

Figure 5 Production blast velocity time histories recorded in (a) rock; and (b) CPB, 24.5 days curing time; 7,580 kg explosive; distances measured from middle of explosive charges; charge weights correspond to each individual blasthole

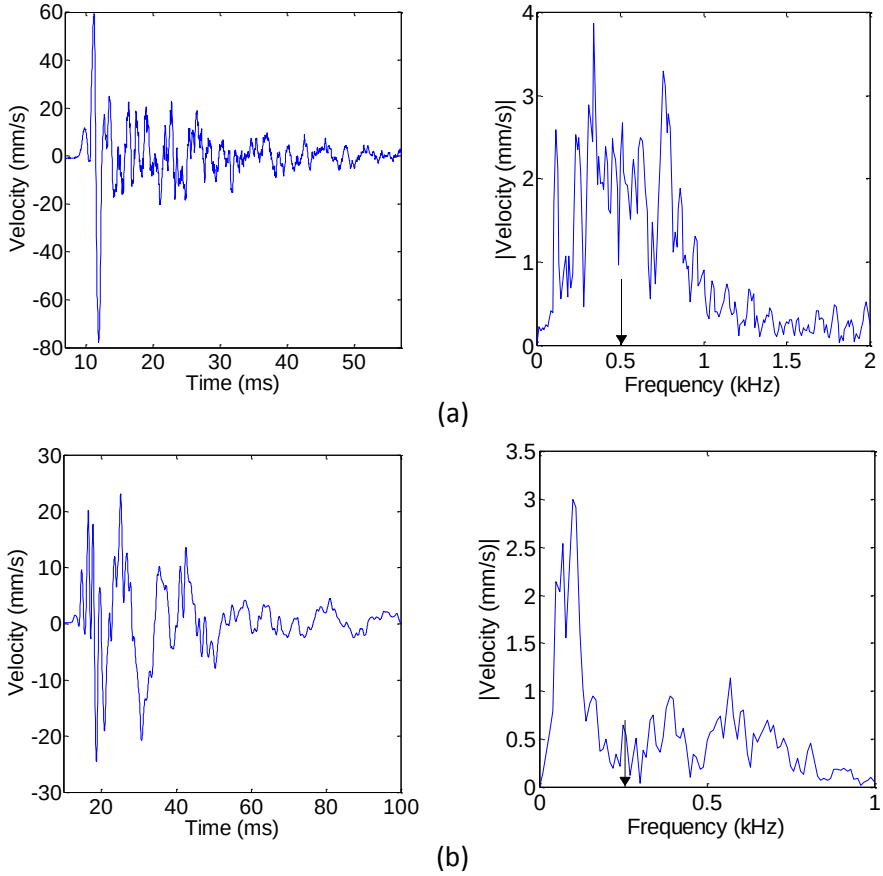

Figure 6 Vibration signature from first hole in production blast (450 kg explosive) (a) rock, 65.9 m distance
source-sensor; (b) CPB, 24.5 day curing time, 72 m distance source-sensor

3.3 Analysis

Figure 7 shows the results of average frequency content in both rock and CPB from control and production blasts. The high dispersion in the measured values does make it difficult to establish a strictly quantitative relation between average frequency content on the one hand and distance and curing time on the other, but a very clear trend can be seen for both with distance and curing time. As expected, the average frequency content in the vibrations drops off rapidly with distance in both host rock and CPB. It is to be noted that in both cases, the frequency content for the control blast is higher due to the relatively short length of the explosive charge. At a distance of 65 m from the blast, the frequency content in the host rock ranges between 300 and 900 Hz, with the average around is about 700 Hz, compared to between 40 and 300 Hz, with the average being about 100 Hz in CPB. A similar but less clear-cut trend is seen for the average frequency content in CPB as a function of curing time, although there is a discernible trend towards higher frequency with curing time.

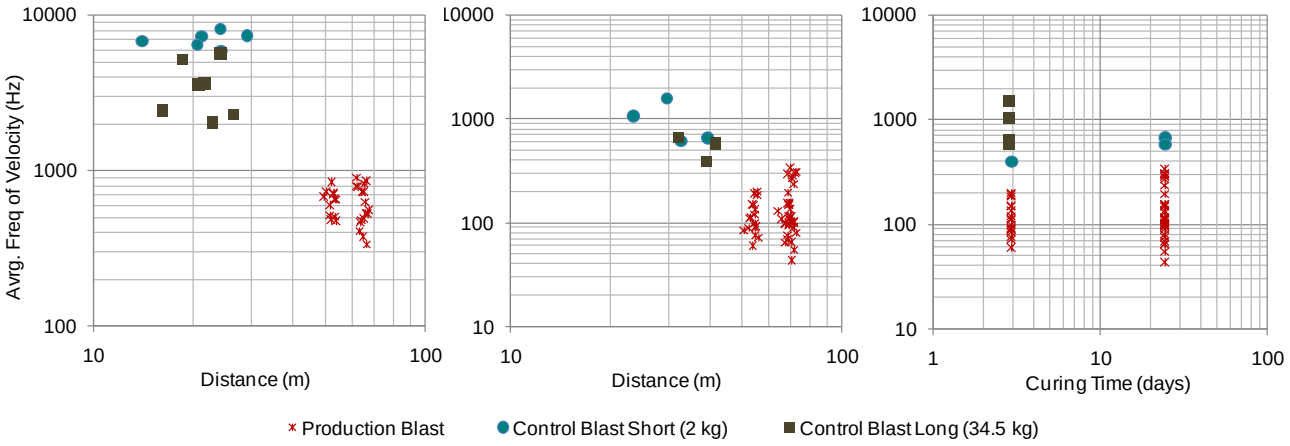

(a) (b) (c)

Figure 7 Average frequency of particle velocity, production and control blasts; (a) rock frequency versus distance; (b) CPB frequency versus distance; (c) CPB frequency versus curing time

Figure 8 shows the results of peak particle velocity, ppv, versus scaled distance, i.e. distance over square root of charge weight, from both single-hole (control) and production blasts. Control blasts in rock clearly show a trend of decreasing ppv with increasing distance, however, production blasts seem to be completely out of this trend, showing much lower amplitudes. This could be due to the possible presence of fractures or faults along the ray paths between the boreholes in question and the rock mass to which the accelerometers were attached, compared to the control blasts. Another contributing factor could be the presence of voids (stopes and drifts) between production blast and sensors, especially due to their location at different levels (Figure 2). For signals recorded in CPB, the trend of decreasing ppv with scaled distance appears to be much more significant, i.e. higher slope, than in rock. Also, in contrast to the signals in rock, production blasts seem to be in line with the trend of control blasts. This difference is likely to be due to the high frequencies generated from control blasts (several kHz) which are responsible for the high amplitudes recorded in rock. These frequencies are significantly attenuated in CPB, which explains the significant drop in amplitude for control blasts. Production blast results, with similar scaled distances, show an increase of ppv versus curing time by about a factor of two from three to 25 days (Figure 8(c)).

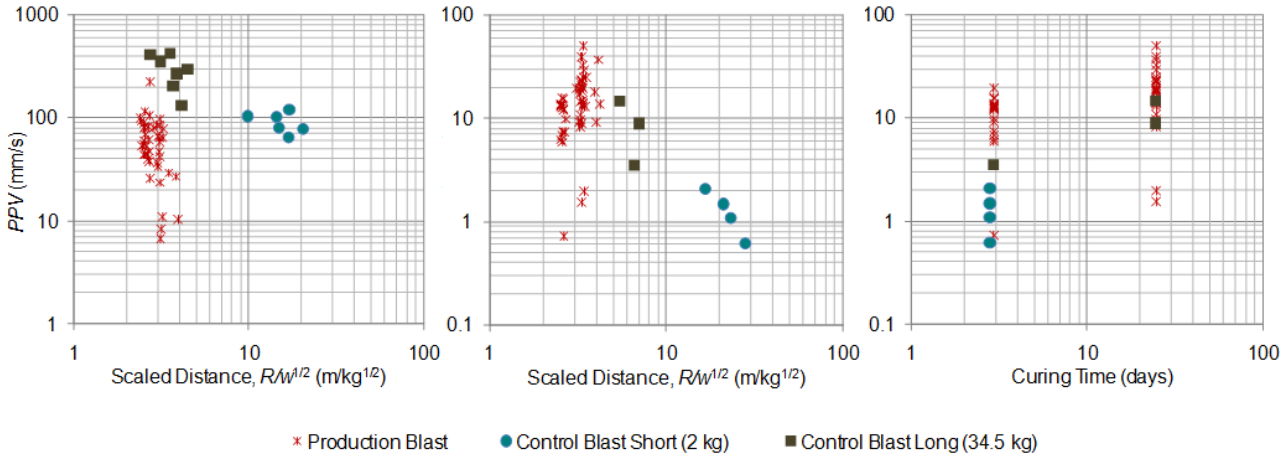

Figure 8 ppv recorded in rock and CPB, production and control blasts; (a) rock frequency versus distance; (b) CPB frequency versus distance; (c) CPB frequency versus curing time

The P-wave velocity in CPB was calculated from measured arrival times of seismic signals and distances travelled by waves through rock and CPB. This was done through an iterative process, as the wave path would change depending on the acoustic mismatch between CPB and rock, which in turn is a function of the P-wave velocities in both materials. For the rock, a P-wave velocity of 5.95 km/s was determined from seismic signals. Figure 10 shows the results of variation of P-wave velocity in CPB as a function of curing time. Although there is considerable scatter in the calculated values, a clear trend of increasing velocity with curing time is observed. The P-wave velocity in CPB after three days of curing is found to average 1 km/s, which steadily increases to 1.6 km/s on the average after 25 days. This is a more clear measure of increasing stiffness in CPB with time.

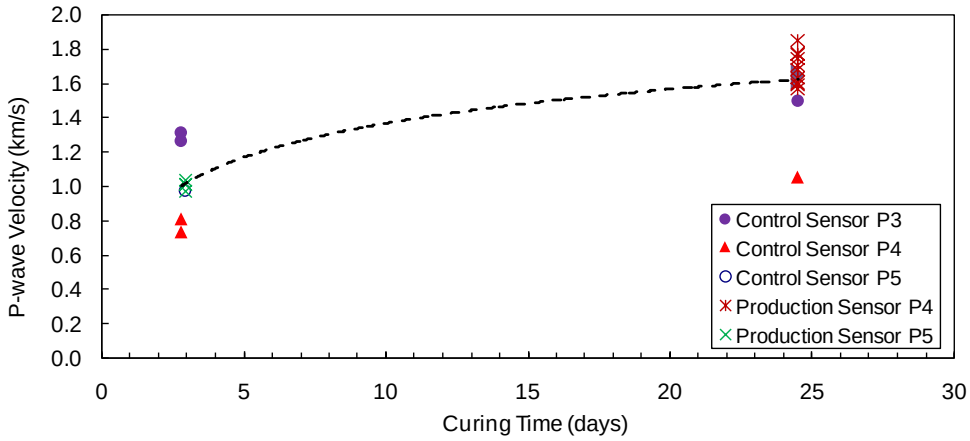

Figure 9 P-wave velocity in CPB versus curing time from control and production blasts

4 Conclusions

A systematic seismic monitoring program has been successfully implemented to characterise the nature of CPB when subjected to dynamic loads arising out of normal production blasting operation. The blasting vibrations represent the dynamic load imposed on CPB. There is significant difference in these loads between the host rock and CFB from blasting operations. From single-hole blasts, the ppv and the frequency content in CPB is shown to be lower by almost two orders of magnitude for the former, and almost an order of magnitude lower in the latter. Vibration monitoring also can be used to track the P–wave velocity change with curing time, and thus the degree of stiffness of CPB with curing time. Within a three week curing period, the P-wave velocity was shown to change from 1 to 1.6 km/s. In addition to

providing regular information on the state of CPB during its curing phase, systematic vibration monitoring within the fill also yields key information on seismic loading rate, and thus serves as a very powerful diagnostic tool for studying health of a CPB. In addition, the measured as well as predicted vibration loads on the backfill can be utilised in calculating the failure limit of the cured backfill, by the standard procedure of calculating the imposed stress due to the particle velocity and the stress wave velocity in the fill. However, additional data, especially on the failure and strength properties of the uncured fill, would be required to utilise the vibration measurements, i.e. amplitude as well as frequency content, as a diagnostic tool, if one were to calculate the failure limit.

Acknowledgement

The authors gratefully acknowledge the financial support provided by the Natural Sciences and Engineering Research Council of Canada (NSERC) during the course of this investigation. We are also grateful to Mr David Counter of Kidd Creek Mine for facilitating the field work, and for the many useful discussions on the subject with Dr Benjamin Thompson and Professor Murray Grabinsky of the University of Toronto.

References

Aref, K 1989, 'A study of the geotechnical characteristics and liquefaction potential of paste backfill', PhD thesis, McGill University.

Been, K, Brown, ET & Hepworth, N 2002, 'Liquefaction potential of paste fill at Neves Corvo mine, Portugal', *Transactions of the Institutions of Mining and Metallurgy*, April 2002, pp. A47-A58.

Grabinsky, M, Bawden, W, Simon, D & Thompson B 2008, 'In situ properties of cemented paste backfill in an alimak stope', *Proceedings of the 61st Canadian Geotechnical Conference and the 9th Joint IAH-CNC/CGS Conference*, Canadian Geotechnical Society, Richmond, pp. 790-6.

Grice, AG 1998, 'Underground mining with backfill', *Proceedings of the 2nd Annual Summit – Mine Tailings Disposal Systems*, pp. 234-9.

Johnson, JC, Williams, T & Pierce, P 2007, 'The response of cemented backfill to dynamic loads from field observations and split Hopkinson pressure bar tests', in FP Hassani and JF Archibald (eds), *Proceedings of the 9th International Symposium on Mining with Backfill*, Canadian Institute of Mining, Metallurgy and Petroleum, Westmount, on CD-ROM.

le Roux, K, Bawden, WF & Grabinsky, MF 2004, 'Liquefaction analysis of early age cemented paste backfill', *Proceedings of the Eighth International Symposium on Mining with Backfill*.

Mohanty, B, Yang, R, LeBlanc, M & Kelly, C 1995, 'Dilution control and vibration studies at an underground mine', *Proceedings of the 25th Annual Conference on Explosives and Blasting Technique*, International Society of Explosives Engineers, Cleveland, pp. 20-29.

Ouellet, J, Benzaazoua, M & Servant, S 1998, 'Mechanical, mineralogical and chemical characterization of a paste backfill', *Proceedings of the 5th International Conference Tailings and Mine Waste*, Balkema, Rotterdam, pp. 139-46.

Revell, M 2000, 'Cannington backfill taking the pig out of paste', *Proceedings of the Paste Technology Seminar*, pp. 1-12.

Saebimoghaddam, A 2010, 'Liquefaction of early age cemented paste backfill', PhD thesis, University of Toronto.

Studer, J & Kok, L 1980, 'Blast-induced excess porewater pressure and liquefaction: Experience and application', in GN Pande & OC Zienkiewicz, *Proceedings of the International Symposium on Soils under Cyclic and Transient Loading*, Balkema, Rotterdam, pp. 581-93.